View Online / Journal Homepage / Table of Contents for this issue
Dynamic Article Links

Organic & Biomolecular Chemistry

Cite this: *Org. Biomol. Chem.*, 2012, **10**, 3841

www.rsc.org/obc

PAPER

Origin of the synchronicity in bond formation in polar Diels–Alder reactions: an ELF analysis of the reaction between cyclopentadiene and tetracyanoethylene

Luis R. Domingo,*[a] Patricia Pérez[b] and Jose A. Sáez[a]

Received 19th January 2012, Accepted 15th March 2012
DOI: 10.1039/c2ob25152c

Published on 15 March 2012 on http://pubs.rsc.org | doi:10.1039/C2OB25152C
Downloaded by Beijing University on 16 June 2012

The origin of the synchronicity in C–C bond formation in polar Diels–Alder (P-DA) reactions involving symmetrically substituted electrophilic ethylenes has been studied by an ELF analysis of the electron reorganization along the P-DA reaction of cyclopentadiene (Cp) **4** with tetracyanoethylene (TCE) **10** at the B3LYP/6-31G* level. The present study makes it possible to establish that the synchronicity in C–C bond formation in P-DA reactions is controlled by the symmetric distribution of the electron-density excess reached in the electrophile through the charge transfer process, which can be anticipated by an analysis of the spin electron-density at the corresponding radical anion. The ELF comparative analysis of bonding along the DA reactions of Cp **4** with ethylene and with TCE **10** asserts that these DA reactions, which have a symmetric electron reorganization, do not have a cyclic electron reorganization as the pericyclic mechanism states. Due to the very limited number of cases of symmetrically substituted ethylenes, we can conclude that the synchronous mechanism is an exception of DA reactions.

Introduction

The Diels–Alder (DA) reaction is arguably one of the most powerful reactions in the arsenal of the synthetic organic chemist.[1] From the discovery of the DA reaction in the 1920s by Otto Diels and Kurt Alder,[2] a tremendous amount of experimental and theoretical work has been devoted to the study of the mechanism and the selectivity of these cycloaddition reactions. Several theories and rules have been proposed in the literature for the study of the reactivity and selectivity of DA reactions, namely the frontier molecular orbital (FMO) theory,[3] the transition state theory (TST),[4] and more recently static reactivity indexes defined within the conceptual density functional theory (DFT).[5]

The first transition state structure (TS) for the DA reaction between butadiene **1** and ethylene **2** was proposed by A. Wassermann in 1935 (see Scheme 1 and Fig. 1a).[6] He suggested that the lengths of the two forming bonds in the symmetric TS were 2.0 Å, a distance close to the 2.3 Å currently obtained (see Fig. 1b). Even today, this symmetric TS is used as the prototype for the DA reaction in all textbooks.

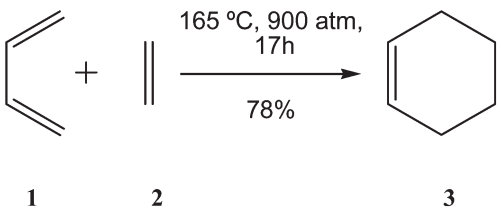

Scheme 1

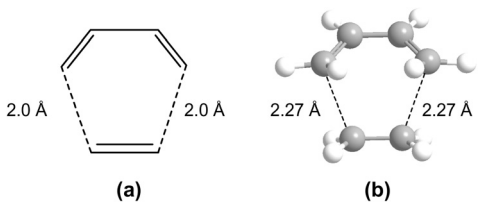

Fig. 1 (a) Wassermann's and (b) B3LYP/6-31G* TSs associated with the known DA reaction between butadiene **1** and ethylene **2**.

However, this DA reaction does not take place easily. For instance, it must be forced to take place: after 17 h at 165 °C and 900 atm, it gives a yield of 78% (see Scheme 1). Presence of electron-releasing substituents in the diene and electron-withdrawing substituents in the dienophile or *vice versa* can drastically accelerate the process. An exhaustive study on the mechanisms of the DA reactions has enabled us to establish a relationship between the activation energy and the polar

[a]*Universidad de Valencia, Departamento de Química Orgánica, Dr. Moliner 50, E-46100 Burjassot, Valencia, Spain. E-mail: domingo@utopia.uv.es*
[b]*Universidad Andrés Bello, Facultad de Ciencias Exactas, Departamento de Ciencias Químicas, Laboratorio de Química Teórica, Av. República 275, 8370146 Santiago, Chile*

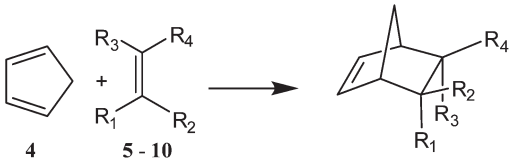

5 $R_1 = CN, R_2 = R_3 = R_4 = H$
6 $R_1 = R_4 = CN, R_2 = R_4 = H$
7 $R_1 = R_3 = CN, R_2 = R_3 = H$
8 $R_1 = R_2 = CN, R_3 = R_4 = H$
9 $R_1 = R_2 = R_3 = CN, R_4 = H$
10 $R_1 = R_2 = R_3 = R_4 = CN$

Scheme 2

Table 1 Experimental rate constants (k), a electrophilicity ω (in eV) index of reagents, and CT (in e) at the TSs associated to the Diels–Alder reactions of Cp (**4**) with ethylene (**2**) and with the cyanoethylene series **5–10**

	k [M^{-1} s^{-1}][a]	ω^b	CT[b]
Ethylene (**2**)	10^{-5}	0.73	0.03
Acrylonitrile (**5**)	1.04	1.74	0.15
trans-1,2-Dicyanoethylene (**6**)	81	3.08	0.24
cis-1,2-Dicyanoethylene (**7**)	91	3.01	0.25
1,1-Dicyanoethylene (**8**)	4.5×10^4	2.82	0.28
Tricyanoethylene (**9**)	4.8×10^5	4.38	0.36
Tetracyanoethylene (**10**)	4.3×10^7	5.96	0.43

[a] Ref. 13. [b] Ref. 12.

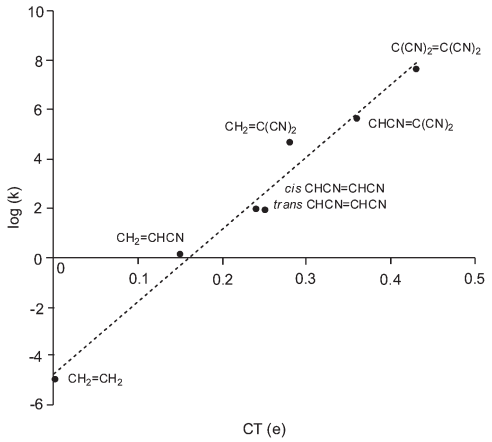

Fig. 2 Plot of the logarithm of the experimental rate constant *vs.* the charge transfer (CT), $R^2 = 0.99$, for the Diels–Alder reactions of Cp **4** with ethylene **2** and with the cyanoethylene series **5–10**.

character of the reaction, measured through the charge transfer (CT) at the TS, allowing for the establishment of the polar Diels–Alder (P-DA) mechanism.[7] Theoretical studies of DA reactions performed using TST have shown that the use of electrophilic asymmetric ethylenes leads to asynchronous TSs.[7,8] In addition, the degree of asynchronicity follows a direct relationship with the polar character of the reaction,[9] which can be anticipated with the analysis of the electrophilicity index ω,[10] defined within the conceptual DFT.[11]

In 2003, we performed a DFT study[12] of the P-DA reactions between cyclopentadiene (Cp) **4** and the series of cyanoethylenes **5–10**, which was studied experimentally by Sauer *et al.* (see Scheme 2).[13] In this series of P-DA reactions, a clear relationship between the experimentally observed acceleration rate[13] and the polar character of the DA reaction was established (see Table 1 and Fig. 2). Both experimental[13] and theoretical[12] studies showed that, while the largest acceleration caused by the cyano substitution corresponds to the DA reaction between Cp and the asymmetrically substituted 1,1-diacyanoethylene (DCE) **8**, the fastest reaction is that with tetracyanoethylene (TCE) **10**, which is the most electrophilic species of this series (see Table 1). Interestingly, while the P-DA reaction of Cp **4** with DCE **8** takes place through a highly asynchronous TS, this reaction with TCE **10** takes place through a synchronous TS that geometrically resembles that of the butadiene **1** with ethylene **2** reaction (see later). We thus concluded that the synchronicity of the C–C bond-formation process can not be related with the reaction rate.[12] Analysis of the local electrophilicity index ω_k[14] of this cyanoethylene series allowed for the establishment of a relationship between the local electrophilic activation of the ethylene carbons and the synchronicity of the reaction. Thus, while DCE **8**, which presents a highly asynchronous TS, has the maximum of ω_k at the non-substituted carbon, *trans* and *cis* 1,2-dicyanoethylenes **6** and **7**, and TCE **10**, which present synchronous TSs, show the same electrophilic activation at the two ethylenic carbons.

Very recently, we have investigated the origin of the asynchronicity in bond formation in polar cycloadditions.[15] An electron localization function[16] (ELF) analysis of bond formation along the 1,3-dipolar cycloaddition of Padwa's carbonyl ylide **11** with the 1,2-benzoquinone **12** (see Scheme 3) established that the C–O bond formation at the carbonyl oxygen atom of benzoquinone **12** anticipates the C–C bond formation. This study established that along a favorable two-center interaction, the bond formation begins at the most electrophilic center, which is the center with the highest excess of electron-density achieved through the CT process, and not, as expected, at the center that presents the larger positive charge.[15]

Recently, we have performed an ELF study of the electron reorganization along the non-polar Diels–Alder (N-DA) reactions between Cp **4** and ethylene **2** and styrene **14**.[17] ELF results for the synchronous mechanism associated with the N-DA reaction between Cp **4** and ethylene **2** stressed that the electron reorganization demanded from the reagents to reach the *pseudodiradical* structures[18] involved in the synchronous C–C bond formation is responsible for the high activation energy (see Fig. 3). It is interesting to remark that at **TSc**, d(C1–C6) = 2.2 Å, no monosynaptic basins appear at the terminal carbon atoms of the reagents (see Fig. 3). The comparative ELF analysis of some relevant points along the intrinsic reaction coordinate (IRC) of these N-DA reactions suggested that the synchronous mechanism, which has a symmetric electron reorganization associated with the formation of the *pseudodiradical* structures, do not have a pericyclic electron reorganization.[17]

Most electrophilically activated ethylenes present asymmetric substitution. Only a few reagents have an ethylenic symmetric substitution. Some of the most experimentally utilized reagents are summarized in Scheme 4. Note that most of them are

Published on 15 March 2012 on http://pubs.rsc.org | doi:10.1039/C2OB25152C
Downloaded by Beijing University on 16 June 2012

 This journal is © The Royal Society of Chemistry 2012

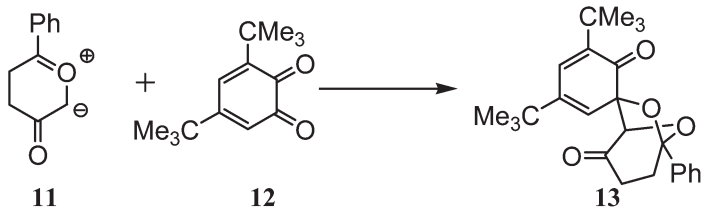

Scheme 3

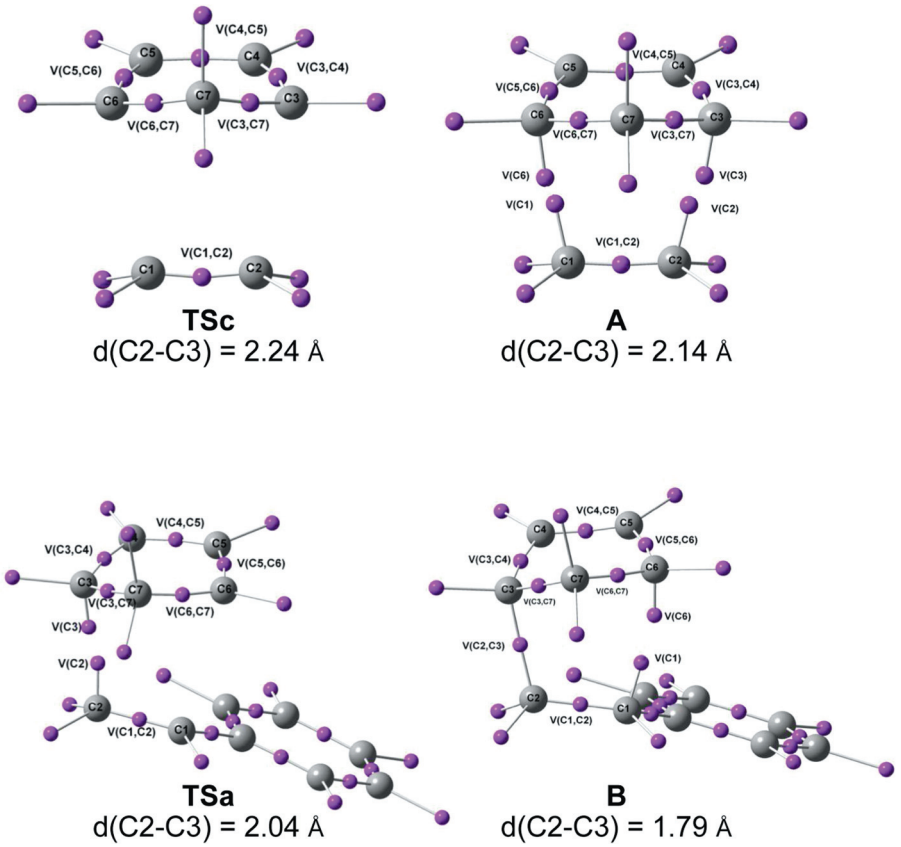

Fig. 3 ELF attractors at selected points of the IRC of the N-DA reaction between Cp **4** and ethylene **2** (top) and between Cp **4** and styrene **14** (bottom).

derivatives of maleic or fumaric acids. Previous theoretical studies devoted to P-DA reactions involving these reagents have indicated that these cycloadditions take place through synchronous bond-formation processes.[19] In spite of the similarity of the geometry of the TSs involved in these P-DA reactions and that associated with N-DA reaction between butadiene and ethylene, the bond-formation process must to have some relevant difference which allows for an explanation of the observed acceleration on P-DA reactions.

In spite of the fact that the analysis of the local electrophilicity at the symmetrically substituted ethylenes allows for a prediction of a synchronous C–C bond-formation process,[12] the origin of these synchronous polar cycloadditions remains unknown. In this study, we present an ELF analysis of the electron reorganization along P-DA reactions involving symmetrically substituted ethylenes, with the aim of establishing the origin of synchronicity of bond formation in polar cycloadditions. With this purpose, the electron reorganization along the reaction channel associated with P-DA reactions between Cp **4** and DCE **8** and TCE **10** is studied by a topological analysis of the ELF along the reaction coordinate.

Computational methods

DFT calculations were carried out using the B3LYP[20] exchange-correlation functionals, together with the standard 6-31G* basis set.[21] The optimisations were carried out using the Berny analytical gradient optimisation method.[22] The stationary points were characterized by frequency calculations in order to verify that TSs have one and only one imaginary frequency. The IRC[23] paths were traced in order to check the energy profiles connecting each TS to the two associated minima of the proposed mechanism using the second order González–Schlegel integration

Published on 15 March 2012 on http://pubs.rsc.org | doi:10.1039/C2OB25152C
Downloaded by Beijing University on 16 June 2012

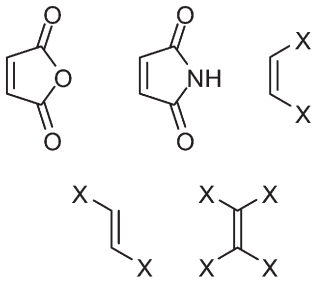

Scheme 4 Some symmetrically substituted electrophilic ethylenes.

Published on 15 March 2012 on http://pubs.rsc.org | doi:10.1039/C2OB25152C
Downloaded by Beijing University on 16 June 2012

method.[24] The electronic structures of stationary points were analyzed by the natural bond orbital (NBO) method[25] and by the topological analysis of the ELF, $\eta(\mathbf{r})$.[16] The ELF study was performed with the TopMod program[26] using the corresponding monodeterminantal wavefunctions of the selected structures of the IRC. All calculations were carried out with the Gaussian 03 suite of programs.[27]

The global electrophilicity index,[10] ω, is given by the following simple expression,[10] $\omega = (\mu^2/2\eta)$, in terms of the electronic chemical potential μ and the chemical hardness η. Both quantities may be approached in terms of the one electron energies of the frontier molecular orbital HOMO and LUMO, ε_H and ε_L, as $\mu \approx (\varepsilon_H + \varepsilon_L)/2$ and $\eta \approx (\varepsilon_L - \varepsilon_H)$, respectively.[28] Associated with the definition of global electrophilicity, there is an additional and useful relationship that accounts for the maximum electronic charge,[10] ΔN_{max}, that the electrophile may accept from the environment. It has been defined as: $\Delta N_{max} = -(\mu/\eta)$. Recently, we have introduced an empirical (relative) nucleophilicity index, N,[29] based on the HOMO energies obtained within the Kohn–Sham scheme,[30] and defined as $N = E_{HOMO}(Nu) - E_{HOMO}(TCE)$. The nucleophilicity is referred to TCE, because it presents the lowest HOMO energy in a large series of molecules already investigated in the context of polar cycloadditions. This choice allows us conveniently to handle a nucleophilicity scale of positive values.[29] Local electrophilicity indices,[31] ω_k, were evaluated using the following expression: $\omega_k = \omega f_k^+$ where f_k^+ is the Fukui function for a nucleophilic attack.[32] Also, the partition for ΔN_{max} is possible in terms of $\Delta N_{max(k)} = \Delta N_{max} f_k^+$.[31]

Results and discussion

In order to understand the origin of the synchronicity in bond formation in P-DA reactions involving symmetrically substituted electrophilic ethylenes, this theoretical study has been divided into four different parts: (i) the mechanistic study of P-DA reactions of Cp **4** with the asymmetrically substituted DCE **8** and the symmetrically substituted TCE **10**; (ii) analysis of these P-DA reactions based on DFT reactivity indices; (iii) ELF analysis of the bond formation along the P-DA reaction between Cp **4** and DCE **8** and TCE **10**, and (iv) analysis of the factors controlling the synchronicity in bond formation in P-DA reactions involving symmetrically substituted electrophilic ethylenes.

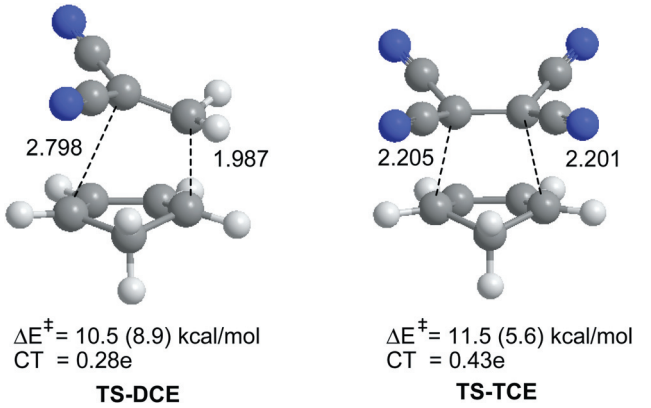

Fig. 4 B3LYP/6-31G* geometries, relative energies and CT in TSs associated with the P-DA reactions between Cp **4** and DCE **8** and TCE **10**. MPW1K/6-31+G** energies in parentheses.

(1) Mechanistic study of the P-DA reaction of Cp 4 with cyanoethylenes DCE 8 and TCE 10

An analysis of the potential energy surface for these P-DA reactions indicates that they correspond to one-step processes.[11] Therefore, two TSs, **TS-DCE** and **TS-TCE**, and their corresponding cycloadducts were located and characterized. The gas-phase B3LYP/6-31G* activation barriers associated with these P-DA reactions are, 10.5 kcal mol^{-1} (**TS-DCE**) and 11.5 kcal mol^{-1} (**TS-TCE**) (see Fig. 4).[12] Further MPW1K/6-31+G** calculations yielded activation barriers close to experimentally estimated values: 8.9 kcal mol^{-1} (**TS-DCE**) and 5.6 kcal mol^{-1} (**TS-TCE**).[33]

The lengths of the C4–C5 and C1–C6 forming bonds at the TSs are 1.987 and 2.798 Å at **TS-DCE**, and 2.201 and 2.205 Å at **TS-TCE**, respectively (see Fig. 4 and Scheme 5).[12] The lengths of the forming C–C bonds for the synchronous **TS-TCE** are closer to those found for the synchronous TS associated with the N-DA reaction between Cp and ethylene **2**, 2.249 and 2.249 Å.[17] The asynchronicity at the TSs, measured by means of the difference between the distances of the two forming bonds, is 0.81 at **TS-DCE** and 0.00 at **TS-TCE**. Therefore, while **TS-DCE** is associated with a highly asynchronous bond-formation process, **TS-TCE** is associated with a synchronous one.

The natural population analysis allows for the evaluation of the CT along these polar cycloadditions. The B3LYP/6-31G* natural atomic charges have been partitioned between Cp **4** and the electron-deficient substituted ethylenes. The negative charge transferred from Cp **4** to the cyanoethylenes is 0.28 *e* at **TS-DCE** and 0.43 *e* at **TS-TCE** (see Fig. 4), thereby indicating that the nature of these TSs may be traced to some zwitterionic character, which increases with the electron-withdrawing substitution. Finally, the synchronous **TSc** associated with the N-DA reaction between Cp **4** and ethylene **2** has a negligible charge transfer, *ca.* 0.0 *e*.[16]

Two main conclusions can be obtained from this analysis at the TSs: (i) there is not any correlation between the synchronicity of a P-DA reactions and its activation energy; while the synchronous DA reaction between Cp **4** and ethylene **2** is one of the most unfavorable DA reactions, that between Cp **4** and TCE **10** is one of the most favorable; (ii) there is a clear relationship

 This journal is © The Royal Society of Chemistry 2012

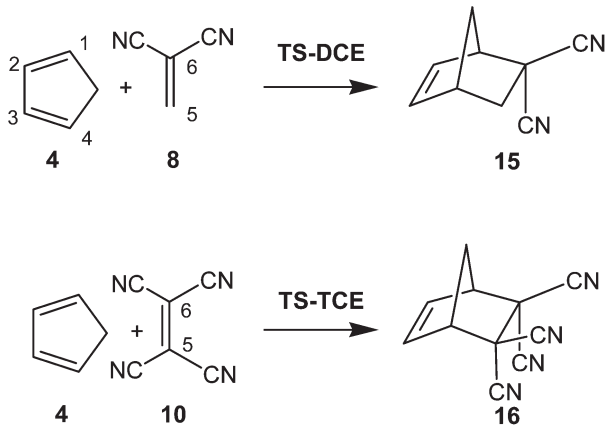

Scheme 5

between the CT and activation energy; the acceleration experimentally observed for the DA reactions of Cp with ethylene **2** and the cyanoethylene series, including DCE **8** and TCE **10**, exhibits a clear linear correlation (see Fig. 2).

(2) Analysis based on DFT reactivity indices

Studies carried out on cycloaddition reactions have shown that the reactivity indices defined within the conceptual DFT are powerful tools for analyzing the polar character of such reactions. The static global properties, electronic chemical potential, μ, chemical hardness, η, global electrophilicity, ω, and global nucleophilicity, N, for ethylene **2**, Cp **4** and the cyanoethylenes DCE **8** and TCE **10** are displayed in Table 2, while the local properties are presented in Table 3.

The electronic chemical potential of cyanoethylenes, −0.21 eV (**8**) and −0.26 eV (**10**), is less than the electronic chemical potential of Cp **4** (μ = −0.11 eV) thereby indicating that the net CT will take place from Cp **4** towards these electron-poor ethylenes. The electrophilicity of cyanoethylenes, ω = 2.82 eV (DCE **8**) and 5.96 (TCE **10**), allows for the classification of these species as strong electrophiles within the electrophilicity scale.[11] On the other hand, Cp **4** presents a high nucleophilic value, N = 3.37 eV, being classified as a strong nucleophile.[34] Therefore, the electrophilicity difference between the diene and dienophile, $\Delta\omega$ = 1.99 eV (DCE **8**/Cp **4**) and 5.13 eV (TCE **10**/Cp **4**), which has been proposed as a measure of the polar character of DA reactions, indicates that these reactions will have a large polar character.[11] The very low value of $\Delta\omega$ for the N-DA reaction between Cp **4** and ethylene **2**, 0.1 eV, agrees with the non-polar character of this reaction.

The local electrophilicity index, ω_k, can be used as a measure of the distribution of the global electrophilicity in the different atomic sites of a molecule. An analysis of ω_k for the asymmetric ethylene DCE **8** shows that the most electrophilic center of the molecule corresponds to the unsubstituted C5 carbon atom of the ethylene, the β-position. However, the symmetric ethylene TCE **10** presents the same electrophilic activation at the two ethylenic carbons. In addition, the $\Delta N_{max}(k)$ index at the C5 center in the asymmetric DCE **8** is even larger than that of the symmetric TCE **10**, the most electrophilic ethylene. Note that the $\Delta N_{max}(k)$ predicts a similar charge distribution at the two ethylenic carbons of TCE **10**.

Two main conclusions can be obtained from this DFT analysis at the ground state of the reagents: (i) the global reactivity indices, namely global electrophilicity, ω, and global nucleophilicity, N, are able to characterize the behaviors of an organic molecule when it participates in a polar reaction; and (ii) the local electrophilicity, ω_k, is able to identify the most electrophilic centers within a molecule. In asymmetrically substituted molecules as DCE **8**, the center having the maximum of ω_k will participate in asynchronous bond-formation processes, whereas in symmetrically substituted molecules as TCE **10**, the symmetric distribution of the maximum of ω_k into the two ethylenic carbons is able to predict a synchronous bond formation.

Table 2 Electronic chemical potential, μ, chemical hardness, η, electrophilicity, ω, and nucleophilicity, N, values, in eV, and ΔN_{max} values of Cp **4** and the cyanosubstituted ethylenes DCE **8** and TCE **10**

	μ	η	ω	N	ΔN_{max}
TCE **10**	−0.26	0.15	5.96	0.00	1.69
DCE **8**	−0.21	0.21	2.82	0.65	1.00
Cp **4**	−0.11	0.20	0.83	3.37	0.55
Ethylene **2**	−0.12	0.29	0.73	1.86	0.43

Table 3 Local electrophilicities, ω_k, in eV, and $\Delta N_{max}(k)$ of cyanosubstituted ethylenes DCE **8** and TCE **10**

	ω_5	$\Delta N_{max}(5)$	ω_6	$\Delta N_{max}(6)$
DCE **8**	0.59	0.21	1.41	0.50
TCE **10**	1.53	0.44	1.53	0.44

(3) ELF bonding analysis along the IRC paths of the P-DA reactions between Cp 4 and DCE 8 and TCE 10

Recent theoretical studies have shown that the topological analysis of the ELF along the reaction path associated with a cycloaddition is a valuable tool for understanding the bonding changes along the reaction path.[35] Consequently, a topology analysis of the ELF along the IRCs of the P-DA reactions between Cp **4** and cyanoethylenes DCE **8** and TCE **10** was performed in order to understand the synchronicity in bond formation in P-DA reactions. The N populations of the more relevant ELF valence basins in different phases along the two IRCs are listed in Tables 4 and 5. A schematic picture of the bonding changes along the different phases involved in these P-DA reactions are given in Fig. 5 and 6, while the attractor positions and atom numbering for the most relevant points are shown in Fig. 7.

Analysis of ELF basin populations along the IRC of the P-DA reaction between Cp **4** and DCE **8** allows for the characterization of ten phases (see Table 4). Phase I, $d1 > 3.37$ Å and $d2 > 3.55$ Å, shows the ELF picture of attractors of the separated reagents. At phase I, two disynaptic basins each one associated with the two C–C double bond of Cp **4**, namely V(C1,C2), V′(C1,C2) and V(C3,C4), V′(C3,C4), whose electronic populations integrate 3.42 e and 3.43 e, respectively, and one

Published on 15 March 2012 on http://pubs.rsc.org | doi:10.1039/C2OB25152C
Downloaded by Beijing University on 16 June 2012

Table 4 Valence basin populations *N* calculated from the ELF of some selected points associated with the asynchronous formation of the C1–C6 and C4–C5 σ bonds along the P-DA reaction between Cp **4** and DCE **8**. The CT along the IRC is also included

	I	II	III	IV	V	VI **TS-DCE**	VII	VIII	IX	X
d(C4–C5)	3.373	2.458	2.388	2.315	2.086	1.987	1.948	1.624	1.605	1.564
d(C1–C6)	3.545	2.990	2.958	2.926	2.835	2.798	2.781	2.375	2.209	1.608
CT	0.03	0.15	0.16	0.18	0.25	0.28	0.29	0.30	0.27	0.14
V(C1,C2)	1.68	1.62	3.26	3.23	3.14	3.04	3.02	2.47	2.31	2.00
V′(C1,C2)	1.74	1.68								
V(C2,C3)	2.21	2.33	2.36	2.38	2.51	2.60	2.64	3.14	1.60	1.70
V′(C2,C3)									1.66	1.82
V(C3,C4)	1.74	3.22	3.20	3.19	2.80	2.63	2.56	2.14	2.08	1.99
V′(C3,C4)	1.69									
V(C5,C6)	1.67	1.59	1.62	3.36	3.18	2.74	2.70	2.12	2.02	1.81
V′(C5,C6)	1.71	1.77	1.74							
V(C5)					0.22	0.37	0.41			
V(C4)					0.32	0.47				
V(C4,C5)							0.53	1.62	1.68	1.80
V(C1)								0.02	0.30	
V(C6)						0.34	0.36	0.72	0.84	
V(C1,C6)										1.75

Published on 15 March 2012 on http://pubs.rsc.org | doi:10.1039/C2OB25152C
Downloaded by Beijing University on 16 June 2012

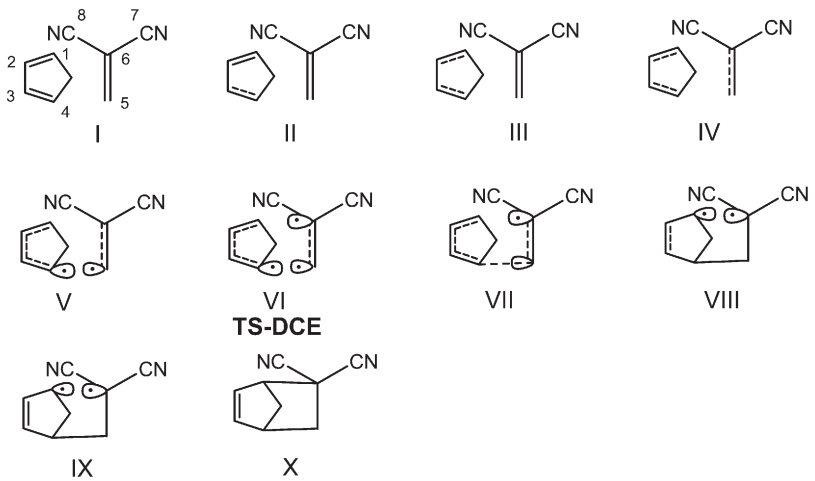

Fig. 5 A schematic representation of disynaptic and monosynaptic basins along the eight phases characterizing the P-DA reaction between Cp **4** and DCE **8**, represented by full lines and by ellipses with a dot, respectively. Dotted over full lines indicate a large basin population, while dotted lines indicate a low basin population.

disynaptic basin corresponding to the central C2–C3 single bond, V(C2,C3), integrating 2.21 *e*, can be distinguished. DCE **8** shows two disynaptic basins associated with the C5–C6 double bond, V(C5,C6) and V′(C5,C6), integrating 3.38 *e*, two disynaptic basins associated with C6–C7 and C6–C8 single bonds, V(C6,C7) and V(C6,C8), integrating 2.22 *e* and 2.29 *e*, respectively, and two disynaptic basins associated with the C–N triple bonds, V(C7,N) and V′(C7,N) and V(C8,N′) and V′(C8,N′), integrating 4.46 *e* each one. Finally, there are two monosynaptic attractors associated with the lone pairs of the terminal nitrogen atoms, V(N) and V(N′), whose electronic population integrates 3.22 *e* and 3.24 *e*, respectively. The attractors associated with the nitrile groups, which change only in population integration along the cycloaddition reaction, will not be discussed or shown in Table 4.

Whereas the two reactants approach each other along phase II, 3.37 > *d*1 > 2.46 Å and 3.55 > *d*2 > 2.99 Å, the two disynaptic basins associated with the C3–C4 double bond of the Cp moiety are merged into each other to become one (*i.e.* V(C3,C4)) with an electronic population of 3.22 *e*. In phase III, 2.46 > *d*1 > 2.39 Å and 2.99 > *d*2 > 2.96 Å, the other pair of disynaptic basins associated with the second C1–C2 double bond of the Cp moiety are also merged into one basin (*i.e.* V(C1,C2)) which integrates to 3.26 *e*. The electronic reorganization of the other attractors mentioned above appears slightly unchanged. In phase IV, 2.39 > *d*1 > 2.32 Å and 2.96 > *d*2 > 2.93 Å, the basins associated with the C5–C6 double bond of the DCE moiety, V(C5,C6) and V′(C5,C6), merge into one basin (*i.e.* V(C5,C6), showing an electronic population of 3.36 *e*.

ELF analysis for phase V, 2.32 > *d*1 > 2.09 Å and 2.93 > *d*2 > 2.84 Å, shows new electronic reorganizations in the moieties of the two reagents: the electronic population of the V(C1,C2) and V(C3,C4) basins of the Cp moiety have asymmetrically decreased to 3.14 *e* and 2.80 *e*, respectively, whereas that of

 This journal is © The Royal Society of Chemistry 2012

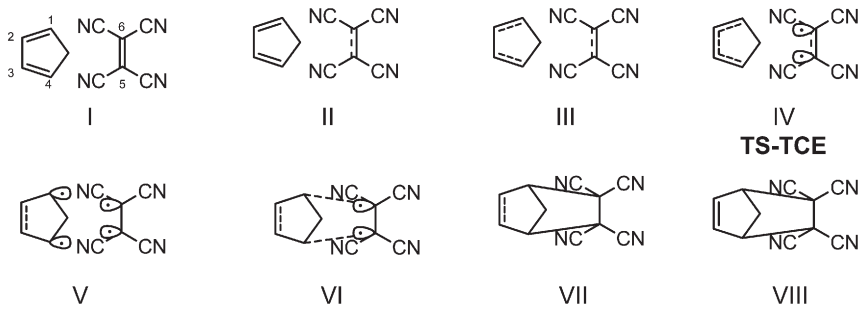

Fig. 6 A schematic representation of disynaptic and monosynaptic basins along the ten phases characterizing the P-DA reaction between Cp **4** and TCE **10**, represented by full lines and by ellipses with a dot, respectively. Dotted over full lines indicate a large basin population, while dotted lines indicate a low basin population.

Published on 15 March 2012 on http://pubs.rsc.org | doi:10.1039/C2OB25152C
Downloaded by Beijing University on 16 June 2012

V(C2,C3) begins to rise to 2.51 *e*. On the other hand, the electronic population of the V(C5,C6) basin decreases to 3.18 *e*. The most interesting changes observed in phase V are the formation of one monosynaptic attractor at the β-conjugated C5 carbon of the DCE moiety, the V(C5) basin, with an electronic population of 0.22 *e*, and the formation of another monosynaptic attractor at the terminal C4 carbon of the Cp moiety, the V(C4) basin, with an electronic population of 0.32 *e*. During this phase, the formation of the first C4–C5 single bond begins to take place.

In phase VI, 2.09 > *d*1 > 1.99 Å and 2.84 > *d*2 > 2.80 Å, a new monosynaptic basin appears at the C6 carbon of the DCE moiety, the V(C6), with an electronic population of 0.34 *e*. ELF analysis for the remaining attractors shows a similar electronic pattern to that found in phase V. In this phase, **TS-DCE** is located at a distance of 1.987 Å between the C4 and C5 carbons, and with a CT from Cp to DCE of 0.28 *e*. Note that this value is identical to that obtained from the NBO analysis, 0.28 *e* (see Fig. 4).

In phase VII, 1.99 > *d*1 > 1.95 Å and 2.80 > *d*2 > 2.78 Å, the most relevant changes along the IRC take place; the V(C4) and V(C5) monosynaptic attractors are merged into one disynaptic attractor to form the V(C4,C5) basin which is associated with the formation of the first C4–C5 single bond of the cycloaddition, with a population of 0.53. Despite this, the V(C5) basin continues to display an electronic population of 0.36 *e*.

Continuing with the ELF analysis along the IRC for this cycloaddition, in phase VIII, 1.95 > *d*1 > 1.62 Å and 2.78 > *d*2 > 2.38 Å, a larger electronic population in the V(C4,C5) basin, 1.62 *e*, which is associated with the more advanced formation of the first C4–C5 single bond, may be seen. The electronic population in the V(C6) basin has grown to 0.72 *e*, and an attractor at C1, namely V(C1), with a minimal electronic population of 0.02 *e* has also begun to appear. At the end of this phase, the C4–C5 bond can be considered formed with a length of 1.624 Å, while the distance between the C1 and C6 remains far, 2.375 Å. In phase VIII the largest CT along the cycloaddition reaction, 0.30 *e*, takes place. Along this phase, it can be seen a consistent decreasing of the electronic population in the V(C1,C2) and V(C3,C4) basins and a increasing of that in the V(C2,C3) basin, which is in agreement with the formation of corresponding single and double bonds along the cycloaddition.

In phase IX, 1.62 > *d*1 > 1.61 Å and 2.38 > *d*2 > 2.21 Å, the electronic populations for V(C1) and V(C6) attractors are increased until they reach a population of 0.30 and 0.84 *e*, respectively. In this phase, the CT of the reaction decreases to 0.27 *e*, probably due to a back-donation from the DCE moiety to that of Cp. At the end of phase IX, while the first C4–C5 single bond has already formed, *d*1 = 1.61 Å, the second C1–C6 single bond has not yet been formed, *d*1 = 2.21 Å. Consequently, this phase shares the two stages of this one-step mechanism.

Finally, in phase X, 1.61 > *d*1 > 1.56 Å and 2.21 > *d*2 > 1.61 Å, both monosynaptic basins V(C1) and V(C6) merge into one disynaptic basin, V(C1,C6), which corresponds with the formation of the second C1–C6 single bond of the cycloaddition. It can be observed that at the end of phase X, the electronic populations in the V(C1,C2) and V(C3,C4) basins are around 2.0 *e*, and the sum for the V(C2,C3) and V′(C2,C3) basins is 3.52 *e*, which is consistent with the C–C single and double bond character, respectively, when the cycloadduct is formed.

Analysis of ELF basin populations along the IRC of the P-DA reaction between Cp **4** and TCE **10** allows for the characterization of eight phases (see Table 5). Phase I, *d* > 3.40 Å, shows the attractors of Cp **4** and TCE **10**. A similar description to that found for the P-DA reaction between Cp **4** and DCE **8** can be seen. In the present case, TCE **10** shows two disynaptic basins associated with the C5–C6 double bond, V(C5,C6) and V′(C5,C6), integrating to 3.39e.

In phase II, 3.40 > *d* > 3.17 Å, as the two reagents approach each other, the two disynaptic attractors of the TCE moiety, V(C5,C6) and V′(C5,C6), merge into each other to become one (*i.e.* V(C5,C6)) with an electronic population of 3.39 *e*. In phase III, 3.17 > *d* > 3.13 Å, something similar but in the Cp moiety occurs: pairs of disynaptic basins associated with the double C1–C2 and C3–C4 bonds of the Cp moiety are also merged into one basin (*i.e.* V(C1,C2) and V(C3,C4)), which integrate 3.30 *e* and 3.31 *e*, respectively.

In phase IV, 3.13 > *d* > 2.21 Å, two monosynaptic basins, V(C5) and V(C6), appear in the TCE moiety, with an electronic population of 0.38 *e* each. It can also be seen that the electronic populations slightly decrease in basins V(C1,C2), V(C3,C4) and V(C5,C6), whereas the electronic population of the V(C2,C3) basin increases slightly. This behavior is expected due to the loss of the double bond character in some bonds and the increase of the double bond character in other bonds. In this phase, **TS-TCE** is located at a distance of 2.21 Å between the C1(4) and C6(5) carbons, and with a CT from Cp to TCE of 0.38 *e*.

In phase V, 2.21 > *d* > 2.08 Å, a new pair of monosynaptic attractors associated with the C1 and C4 carbons of the Cp

Table 5 Valence basin populations *N* calculated from the ELF of some selected points associated with the synchronous formation of the C1–C6 and C4–C5 σ bonds along the P-DA reaction between Cp **4** and TCE **10**. The CT along the IRC is also included

	I	II	III	IV **TS-TCE**	V	VI	VII	VIII
d(C1(4)–C6(5))	3.400	3.174	3.133	2.206	2.084	2.069	1.980	1.609
CT	0.10	0.13	0.14	0.38	0.44	0.44	0.43	0.29
V(C1,C2)	1.76	1.65	3.30	2.95	2.40	2.38	2.28	2.01
V′(C1,C2)	1.62	1.65						
V(C2,C3)	2.22	2.24	2.25	2.59	3.04	3.05	3.16	1.69
V′(C2,C3)								1.78
V(C3,C4)	1.74	1.66	3.31	2.95	2.39	2.37	2.28	2.02
V′(C3,C4)	1.62	1.65						
V(C5,C6)	1.65	3.39	3.38	2.76	2.24	2.24	2.11	1.85
V′(C5,C6)	1.74							
V(C1)					0.32			
V(C4)					0.32			
V(C5)				0.38	0.79	0.33		
V(C6)				0.38	0.78	0.34		
V(C1,C6)						0.80	1.28	1.76
V(C4,C5)						0.81	1.29	1.76

Published on 15 March 2012 on http://pubs.rsc.org | doi:10.1039/C2OB25152C
Downloaded by Beijing University on 16 June 2012

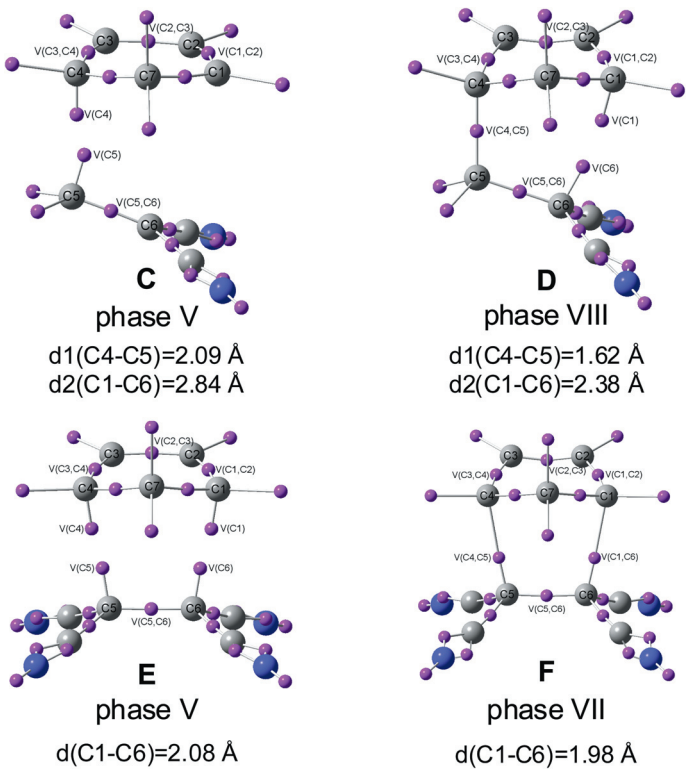

Fig. 7 ELF attractors at selected points of the IRC of the P-DA reactions between Cp **4** and DCE **8** (top) and TCE **10** (bottom).

moiety appear, the V(C1) and V(C4) basins, with a symmetric integration of 0.32 *e*. The other pair of V(C5) and V(C6) monosynaptic attractors associated to the TCE moiety symmetrically increases its electronic population to 0.78 *e*. A similar pattern to that discussed in the above phase for V(C1,C2), V(C3,C4), V(C5,C6) and that for V(C2,C3) is found in phase IV. At the end of this phase, the CT from Cp to TCE rises to 0.44 *e*. It is interesting to note that points belonging to phases IV and V have similar attractor pictures to those found in phases IV and V of the N-DA reaction between butadiene **1** and ethylene **2**.[35a]

In phase VI, 2.08 > *d* > 2.07 Å, monosynaptic attractors V(C1) and V(C6), and the other ones, V(C4) and V(C5), are merged into two disynaptic attractors, V(C1,C6) and V(C4,C5), respectively, with an electronic population of 0.80 *e* and 0.81 *e*, respectively. These disynaptic attractors are associated with the formation of the two new single C–C bonds along the cycloaddition. A similar pattern to that of the P-DA reaction of Cp **4** with DCE **8** is observed: two monosynaptic attractors, V(C5) and V(C6) associated with the TCE moiety still keep an electronic population of 0.33e and 0.34e, respectively.

 This journal is © The Royal Society of Chemistry 2012

Published on 15 March 2012 on http://pubs.rsc.org | doi:10.1039/C2OB25152C
Downloaded by Beijing University on 16 June 2012

In phase VII, 2.07 > d > 1.98 Å, the aforementioned monosynaptic basins disappear and the electronic population in the attractors assigned to the bond region, V(C1,C6) and V(C4,C5), increase to 1.28 e. Population of the V(C2,C3) disynaptic basin begins to increase, whereas the population of V(C1,C2), V(C3,C4) and V(C5,C6) disynaptic ones decreases.

Finally, in phase VIII, 1.98 > d > 1.61 Å, a split of the disynaptic basin V(C2,C3) into two disynaptic basins V(C2,C3) and V′(C2,C3), integrating 1.69 and 1.78 e, respectively, is observed. This behavior accounts for the formation of the C2–C3 double bond at the corresponding cycloadduct.

The present ELF analysis corroborates the early observation obtained from the geometrical and electronic analysis at **TS-DCE** and **TS-TCE**: while along the approach of Cp **4** towards the asymmetrically substituted DCE **8**, the bond formation begins at the most electrophilically activated β-conjugated C5 carbon of DCE **8**, along the approach of Cp **4** towards the symmetrically substituted TCE **10**, the bond formations take place concurrently at the two ethylene C5 and C6 carbons of TCE **10**.

A comparison of the ELF attractors at phases V and VIII of the P-DA reaction between Cp **4** and DCE **8** (see Fig. 5), and phases V and VII of the P-DA reaction between Cp **4** and TCE **10** (see Fig. 6) with those associated with the N-DA reaction between Cp **4** and ethylene **2** and between Cp **4** and styrene **14** (see Fig. 3),[17] shows great similitude. Consequently, the large stabilization observed in P-DA reactions relative to the N-DA reactions can be associated with the large CT found in the polar processes, which enables the C–C bond formation through *zwitterionic pseudodiradical* structures.[36] These comparative studies also allow assertion that the N-DA reactions between Cp **4** and ethylene **2** and the P-DA reaction between Cp **4** and TCE **10**, which take place through synchronous TSs, do not have a cyclic electron reorganization as the pericyclic mechanism indicates, but a symmetric electron reorganization along the plane of symmetry that the Cp **4** and ethylene **2** and TCE **10** molecules share along the C2–C3 and C5–C6 bonds. These symmetric changes, visualized in Fig. 6, are demanded to reach the *pseudodiradical* structures shown in Fig. 3 and 7, which open the subsequent synchronous bond formation.

(4) Factors controlling the synchronicity in the C–C bond formation in P-DA reactions

What is the origin of the synchronicity in the bond formation in P-DA reactions involving symmetrically substituted electrophiles? ELF analysis along the reaction path associated with the P-DA reaction between Cp **4** and the symmetrically substituted TCE **10** shows a synchronous C–C bond formation. Point **E** at d = 2.08 Å belonging to phase V (see Fig. 7) presents a similar ELF attractor pattern than that found at point **A** at d = 2.14 Å of the N-DA reaction between Cp **4** and ethylene **2** (see Fig. 3), which was characterized as a *pseudodiradical* species.[17] However, these structures present two substantial differences: (i) while point **E** is located 8.6 kcal mol^{-1} above the separated reagents, point **A** is located 18.2 kcal mol^{-1} above of the reagents; that is, point **E** has an electronic stabilization of 8.6 kcal mol^{-1} relative to point **A** (note that stabilization reaches 16.0 kcal mol^{-1} at the MPW1K/6-31+G** level); and (ii) while at point **E** the CT is 0.44 e, it is negligible at point **A**, 0.00 e. Consequently, the large stabilization of point **E**, which can be associated to a *zwitterionic pseudodiradical* species, can be related to the large CT that takes place in the polar mechanism.

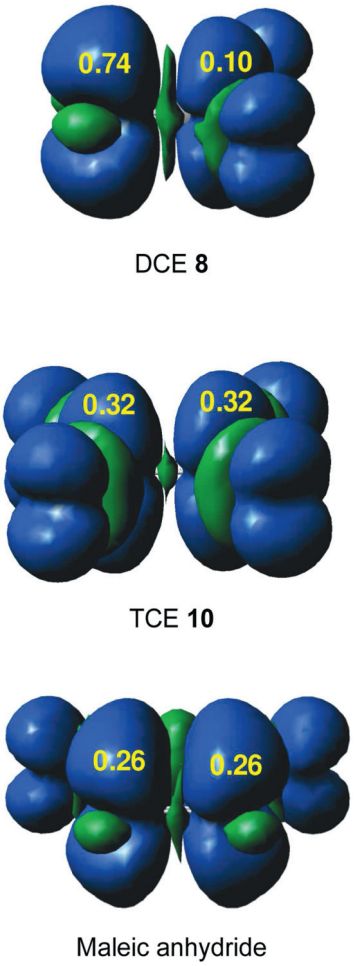

Fig. 8 Atomic spin densities (ASDs) of anion radicals of DCE **8**, TCE **10** and maleic anhydride.

In the extreme case of transferring an amount of an electron-density equivalent to one electron, TCE **10** becomes a radical anion. Analysis of the atomic spin density (ASD) at the radical anion of TCE **10** indicates that it is symmetrically distributed at the two ethylenic C5 and C6 carbons, 0.32 (see Fig. 8). Note that in the radical anion of DCE **8**, the ASD is mainly concentrated at the non-substituted C5 carbon, 0.74, which corresponds to the most electrophilic center of DCE **8** (see Fig. 8). It is interesting to note that the populations found in the V(5) and V(6) monosynaptic basins in the asymmetric **TS-DCE** and the symmetric **TS-TCE** correlate well with the ASD distribution at the radical anions of DCE **8** and TCE **10**. Consequently, the symmetric distribution of the electron-density excess in the TCE moiety achieved through the CT process along the polar cycloaddition is responsible for the synchronicity in the C–C bond formation. Note that a similar ASD distribution is found at the radical anion of maleic anhydride (see Fig. 8), which also participates in P-DA reactions *via synchronous* TSs.[19]

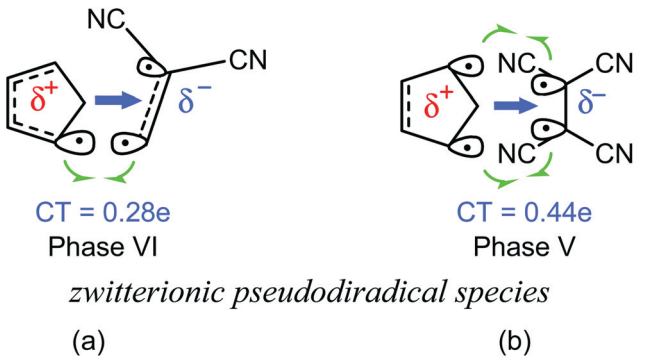

Fig. 9 Schematic representation of the CT from the nucleophile to the electrophile (blue bold arrow) and C-to-C *pseudodiradical* coupling (single-headed green arrows) along the C–C bond formation in the P-DA reactions between Cp **4** and (a) DCE **8** and (b) TCE **10**.

Published on 15 March 2012 on http://pubs.rsc.org | doi:10.1039/C2OB25152C
Downloaded by Beijing University on 16 June 2012

Consequently, it seems that along a polar cycloaddition, the CT that takes place from the nucleophile towards the electrophile favours the electron reorganisation needed to reach the formation of the monosynaptic basins in both the nucleophile and the electrophile. In the case of symmetrically substituted ethylenes such as TCE **10** and those shown in Scheme 4, the symmetric distribution of the electron-density excess at the two ethylenic carbons may favour the synchronous C–C bond formation, while in the case of asymmetrically substituted ethylenes such as DCE **8**, the asynchronous bond formation begins at the most electrophilic center, which corresponds to the center of maximum electron-density accumulation reached in the electrophilic species through the CT process (see Fig. 9).[15]

Conclusions

The origin of the synchronicity in bond formation in P-DA reactions has been studied by an ELF comparative analysis of the electron reorganization along the P-DA reactions of Cp **4** with DCE **8** and TCE **10** at the B3LYP/6-31G* level. These reactions, which have a one-step mechanism, present a different synchronicity in bond formation, controlled by the location of the most electrophilic centers in these substituted ethylenes. Thus, while DCE **8**, which has the most electrophilic center at the β-conjugated position, presents a high C–C asynchronous bond formation, TCE **10**, which has a symmetric electrophilic activation at the two ethylenic carbons, presents a synchronous C–C bond formation.

This study makes it possible to the establish that the synchronicity in bond formation in P-DA reactions is controlled by the symmetric distribution of the electron-density excess reached in the electrophilic species through the CT process, which can be anticipated by an analysis of the spin electron-density at the corresponding radical anion.

The ELF analysis of bonding along the N-DA reactions between Cp **4** and ethylene **2** and the P-DA reaction between Cp **4** and TCE **10** allows for the establishment that these DA reactions, which have a symmetric electron reorganization along the plane of symmetry dividing the Cp **4** and ethylene **2** and TCE **10** molecules along the C2–C3 and C5–C6 bonds, do not have a cyclic electron reorganization as the pericyclic mechanism states. Finally, due to a very limited number of cases of symmetrically substituted electrophilic ethylenes, we can conclude that the synchronous mechanism is an exception among the DA reactions.

Acknowledgements

We are grateful to the Spanish Government (project CTQ2009-11027/BQU), and the Fondecyt project No. 1100278. Professor Domingo thanks Fondecyt for their support through the Cooperación Internacional.

References

1 (*a*) W. Carruthers, *Some Modern Methods of Organic Synthesis*, Cambridge University Press, Cambridge, 1978; (*b*) W. Carruthers, *Cycloaddition Reactions in Organic Synthesis*, Pergamon, Oxford, 1990.
2 O. Diels and K. Alder, *Justus Liebigs Ann. Chem.*, 1928, **460**, 98.
3 K. Fukui, *Molecular Orbitals in Chemistry, Physics, and Biology*, New York, 1964.
4 (*a*) H. Eyring and M. Z. Polanyi, *Phys. Chem. Abt. B*, 1931, **12**, 279; (*b*) H. Eyring, *Chem. Rev.*, 1935, **17**, 65–77; (*c*) K. J. Laidler and M. C. King, *J. Phys. Chem.*, 1983, **87**, 2657–2664.
5 (*a*) P. Geerlings, F. De Proft and W. Langenaeker, *Chem. Rev.*, 2003, **103**, 1793–1873; (*b*) D. H. Ess, G. O. Jones and K. N. Houk, *Adv. Synth. Catal.*, 2006, **348**, 2337–2361.
6 A. Wasserman, *Diels–Alder Reactions*, New York, 1965.
7 L. R. Domingo and J. A. Sáez, *Org. Biomol. Chem.*, 2009, **7**, 3576–3583.
8 Synchronous or asynchronous processes can be related to the extension of bond formation of the two C–C σ bonds that are being formed in a cycloaddition reaction. While in a synchronous process the two new σ bonds are formed to the same extent, in an asynchronous process formation of one σ bond is advanced with respect to the other.
9 L. R. Domingo, M. Arnó and J. Andrés, *J. Org. Chem.*, 1999, **64**, 5867–5875.
10 R. G. Parr, L. von Szentpaly and S. Liu, *J. Am. Chem. Soc.*, 1999, **121**, 1922–1924.
11 L. R. Domingo, M. J. Aurell, P. Pérez and R. Contreras, *Tetrahedron*, 2002, **58**, 4417–4423.
12 L. R. Domingo, M. J. Aurell, P. Pérez and R. Contreras, *J. Org. Chem.*, 2003, **68**, 3884–3890.
13 J. Sauer, H. Wiest and A. Mielert, *Chem. Ber.*, 1964, **97**, 3183–3207.
14 L. R. Domingo, M. J. Aurell, P. Pérez and R. Contreras, *J. Phys. Chem. A*, 2002, **106**, 6871–6875.
15 L. R. Domingo, M. J. Aurell, P. Pérez and J. A. Sáez, *RSC Adv.*, 2012, **2**, 1334–1342.
16 (*a*) A. Savin, A. D. Becke, J. Flad, R. Nesper, H. Preuss and H. G. Vonschnering, *Angew. Chem., Int. Ed. Engl.*, 1991, **30**, 409–412; (*b*) A. Savin, B. Silvi and F. Colonna, *Can. J. Chem.*, 1996, **74**, 1088–1096; (*c*) A. Savin, R. Nesper, S. Wengert and T. F. Fassler, *Angew. Chem., Int. Ed. Engl.*, 1997, **36**, 1808–1832; (*d*) B. Silvi, *J. Mol. Struct.*, 2002, **614**, 3–10.
17 L. R. Domingo, E. Chamorro and P. Pérez, *Org. Biomol. Chem.*, 2010, **8**, 5495–5504.
18 In 1960 Errede *et al.* studied the high chemical reactivity of *p*-xylylene, which was attributed to its *pseudodiradical* character. They defined a *pseudodiradical* as a diamagnetic compound that behaves chemically as if were a diradical. L. A. Errede, J. M. Hoyt and R. S. Gregorian, *J. Am. Chem. Soc.*, 1960, **53**, 5224–5227.
19 (*a*) A. Arrieta, F. P. Cossio and B. Lecea, *J. Org. Chem.*, 2001, **66**, 6178–6180; (*b*) J. I. Garcia, J. A. Mayoral and L. Salvatella, *Eur. J. Org. Chem.*, 2005, 85–90.
20 (*a*) A. D. Becke, *J. Chem. Phys.*, 1993, **98**, 5648–5652; (*b*) C. Lee, W. Yang and R. G. Parr, *Phys. Rev. B*, 1988, **37**, 785–789.
21 W. J. Hehre, L. Radom, P. v. R. Schleyer and J. A. Pople, *Ab initio Molecular Orbital Theory*, Wiley, New York, 1986.
22 (*a*) H. B. Schlegel, *J. Comput. Chem.*, 1982, **3**, 214–218; (*b*) H. B. Schlegel, Geometry Optimization on Potential Energy Surface,

 This journal is © The Royal Society of Chemistry 2012

View Online

in *Modern Electronic Structure Theory*, ed. D. R. Yarkony, World Scientific Publishing, Singapore, 1994.
23 K. Fukui, *J. Phys. Chem.*, 1970, **74**, 4161–4163.
24 (*a*) C. González and H. B. Schlegel, *J. Phys. Chem.*, 1990, **94**, 5523–5527; (*b*) C. González and H. B. Schlegel, *J. Chem. Phys.*, 1991, **95**, 5853–5860.
25 (*a*) A. E. Reed, R. B. Weinstock and F. Weinhold, *J. Chem. Phys.*, 1985, **83**, 735–746; (*b*) A. E. Reed, L. A. Curtiss and F. Weinhold, *Chem. Rev.*, 1988, **88**, 899–926.
26 S. Noury, X. Krokidis, F. Fuster and B. Silvi, *Comput. Chem.*, 1999, **23**, 597–604.
27 M. J. Frisch, G. W. Trucks, H. B. Schlegel, G. E. Scuseria, M. A. Robb, J. R. Cheeseman, J. Montgomery, J. A. T. Vreven, K. N. Kudin, J. C. Burant, J. M. Millam, S. S. Iyengar, J. Tomasi, V. Barone, B. Mennucci, M. Cossi, G. Scalmani, N. Rega, G. A. Petersson, H. Nakatsuji, M. Hada, M. Ehara, K. Toyota, R. Fukuda, J. Hasegawa, M. Ishida, T. Nakajima, Y. Honda, O. Kitao, H. Nakai, M. Klene, X. Li, J. E. Knox, H. P. Hratchian, J. B. Cross, C. Adamo, J. Jaramillo, R. Gomperts, R. E. Stratmann, O. Yazyev, A. J. Austin, R. Cammi, C. Pomelli, J. W. Ochterski, P. Y. Ayala, K. Morokuma, G. A. Voth, P. Salvador, J. J. Dannenberg, V. G. Zakrzewski, S. Dapprich, A. D. Daniels, M. C. Strain, O. Farkas, D. K. Malick, A. D. Rabuck, K. Raghavachari, J. B. Foresman, J. V. Ortiz, Q. Cui, A. G. Baboul, S. Clifford, J. Cioslowski, B. B. Stefanov, G. Liu, A. Liashenko, P. Piskorz, I. Komaromi, R. L. Martin, D. J. Fox, T. Keith, M. A. Al-Laham, C. Y. Peng, A. Nanayakkara, M. Challacombe, P. M. W. Gill, B. Johnson, W. Chen, M. W. Wong, C. Gonzalez and J. A. Pople, *Gaussian03*, 2004.
28 (*a*) R. G. Parr and R. G. Pearson, *J. Am. Chem. Soc.*, 1983, **105**, 7512–7516; (*b*) R. G. Parr and W. Yang, *Density Functional Theory of Atoms and Molecules*, Oxford University Press, New York, 1989.
29 (*a*) L. R. Domingo, E. Chamorro and P. Pérez, *J. Org. Chem.*, 2008, **73**, 4615–4624; (*b*) L. R. Domingo and P. Pérez, *Org. Biomol. Chem.*, 2011, **9**, 7168–7175.
30 W. Kohn and L. J. Sham, *Phys. Rev.*, 1965, **140**, 1133–1138.
31 L. R. Domingo, M. J. Aurell, P. Pérez and R. Contreras, *J. Phys. Chem. A*, 2002, **106**, 6871–6875.
32 R. Contreras, P. Fuentealba, M. Galván and P. Pérez, *Chem. Phys. Lett.*, 1999, **304**, 405–413.
33 G. O. Jones, V. A. Guner and K. N. Houk, *J. Phys. Chem. A*, 2006, **110**, 1216–1224.
34 P. Jaramillo, L. R. Domingo, E. Chamorro and P. Pérez, *J. Mol. Struct. (THEOCHEM)*, 2008, **865**, 68–72.
35 (*a*) S. Berski, J. Andrés, B. Silvi and L. R. Domingo, *J. Phys. Chem. A*, 2003, **107**, 6014–6024; (*b*) V. Polo, J. Andrés, R. Castillo, S. Berski and B. Silvi, *Chem.–Eur. J.*, 2004, **10**, 5165–5172; (*c*) L. R. Domingo, M. T. Picher, P. Arroyo and J. A. Sáez, *J. Org. Chem.*, 2006, **71**, 9319–9330; (*d*) S. Berski, J. Andrés, B. Silvi and L. R. Domingo, *J. Phys. Chem. A*, 2006, **110**, 13939–13947; (*e*) V. Polo, J. Andrés, S. Berski, L. R. Domingo and B. Silvi, *J. Phys. Chem. A*, 2008, **112**, 7128–7136; (*f*) L. R. Domingo, E. Chamorro and P. Pérez, *Lett. Org. Chem.*, 2010, **7**, 432–439; (*g*) L. R. Domingo and J. A. Sáez, *J. Org. Chem.*, 2011, **76**, 373–379.
36 A *zwitterionic pseudodiradical* species is a *pseudodiradical* which presents a charge separation between two fragments of the species.

Published on 15 March 2012 on http://pubs.rsc.org | doi:10.1039/C2OB25152C
Downloaded by Beijing University on 16 June 2012